

Transient Liquid Jet Breakup Model and Comparison with Phase Doppler Measurements

Sang Ku Chang*, Ja Ye Koo**, Hong Chul Chung***

(Received April 25, 1994)

A new liquid jet breakup model is developed based on the transient breakup mechanism and incorporated into the KIVA-II code. Liquid column is considered as a chain of balls. Rayleigh-Taylor instability and Kelvin-Helmholtz instability was applied to the liquid jet column. Liquid jet column is continuously surveyed to apply breakup mechanisms. Once liquid droplets are separated from the main liquid jet column, these droplets are subjected to the single breakup mechanism. When Bond number is greater than a critical Bond number, single droplets continue to break up by Rayleigh-Taylor instability or Kelvin-Helmholtz instability. Computational results were compared with the PDPA measurement data. Gross behavior of the spray and detailed droplet sizes and velocities predicted by KIVA calculations which include proposed drop breakup model are compared with those produced from droplet size/velocity measurements.

Key Words: Breakup Model, Rayleigh-Taylor Instability, PDPA Measurement

1. Introduction

Direct injection engines have been demonstrated the potential for improved fuel economy and reduced fuel sensitivity. Better understanding of atomization process and breakup mechanisms is necessary to achieve optimum fuel distribution in combustion chamber the low pollutant emissions and high performance. Since combustion is strongly influenced by the details of fuel spray in diesel engines, there have been many experimental and theoretical studies on fuel sprays. The mechanism of fuel injection process has not been completely clarified due to the complexity of this process and the difficulties in experiments. However, newly proposed models for physical mecha-

nisms of a jet spray atomization and recent advances in laser diagnostic techniques for measurements of droplet size and velocity are providing opportunities to the better understanding of injection and combustion process.

Even though atomizing diesel fuel sprays have been studied extensively for several decades, the mechanism of atomization is still not well understood because of complex phenomena involved in the process. These include breakup, disintegration, atomization, collision and coalescence. There are several mechanisms for atomization of diesel fuel. Some of the spray behavior can be explained by aerodynamic interaction effects, liquid turbulence, cavitation, jet velocity profile rearrangement effects, and liquid-supply pressure oscillations(Reitz, 1978). Among these mechanisms, Ruiz and Chigier(1985) took the first three mechanisms as the most likely mechanisms. But Reitz(1978) showed that none of the above breakup mechanisms were sufficient to explain completely the observed phenomena.

Here we will focus on jet breakup and droplet breakup caused by hydrodynamic forces to develop a liquid jet breakup model, and subse-

* Ministry of Science and Technology, 1, Jungang-dong, Gwacheon 427-010, Korea

** Department of Aeronautical and Mechanical Engineering, Hankuk Aviation University, 200-1, Hwajon-dong, Koyang-shi, Kyungki-do 411-791, Korea

*** Department of Aerospace Engineering, Hankuk Aviation University, 200-1, Hwajon-dong, Koyang-shi, Kyungki-do 411-791, Korea

quently incorporating the breakup model into KIVA-II computer code and comparison with measurements of droplets sizes and velocities in diesel fuel spray. The measured data are also compared with stability criteria.

2. Transient Breakup Model

2.1 Breakup model

Liquid jet breakup is the result of competing, unstable hydrodynamic forces acting on the liquid jet. Liquid jet breakup regimes can be divided into Rayleigh, laminar-turbulent transition, turbulent, and jet atomization regime depending on jet velocity (Bower et al., 1988). General liquid jet breakup length curve as a function of jet velocity and the corresponding regimes can be found in the literature (Bower et al., 1988). High speed jet through a diesel nozzle into a high pressure chamber belongs to atomization regime. Atomization regime (Hiroyasu et al., 1990) is divided into complete spray regime and incomplete spray regime depending on whether or not deformation process of the liquid column vanished. As Reynolds number increase in the atomization regime, liquid column is disintegrated directly due to internal factors which may be originated from turbulences and/or cavitations inside a nozzle. Breakup in the atomization regime is thought to be a result of aerodynamic forces and jet-flow/nozzle conditions.

Aerodynamic theory involves unstable wave growth on the liquid jet surface, on ligaments, or on the windward surface of larger droplets that initially broke off from the main liquid jet. The surface wave perturbation grows with time, driven by the Kelvin-Helmholtz instability (Chandrasekhar, 1971), or the Rayleigh-Taylor instability (Taylor, 1963a, b).

The Kelvin-Helmholtz (*K-H*) instability arises due to a relative shearing motion at a common interface of a two fluids where one fluid flows over another. Ligament and droplet detachments from the surface are brought about by the fastest growing of the unstable surface waves. Droplet sizes are related to the unstable wave length.

The Rayleigh Taylor (*R-T*) instability occurs

in the fluid interface when a body force is directed from more dense fluid to the less dense fluid. Any perturbation of this interface tends to grow with time. A liquid sheet (or drop) which is being accelerated by air pressure acting on its surface is subject to possible *R-T* instability at the sheet (or drop) windward surface.

When a liquid sheet which has uniform thickness is accelerated by air pressure acting on its upper surface (lighter density ρ_1), the behavior of the upper surface of a sheet of heavier density ρ_2 can be described by *R-T* instability. The disturbance on the unstable fluid surface for a vertical downward acceleration at any time is given as follows (Taylor, 1963b),

$$\eta = \eta_0 \cosh \left\{ -k(g_1 - g) \frac{(\rho_2 - \rho_1)}{(\rho_2 + \rho_1)} \right\}^{\frac{1}{2}} t \quad (1)$$

where η_0 is initial amplitude of the disturbance, k is wave number ($k = 2\pi/\lambda$), g_1 is vertical downward acceleration and g is the acceleration due to gravity. If the liquid sheet moves downward a distance s during the acceleration,

$$\eta = \eta_0 \cosh \sqrt{\left\{ 2ks \frac{(g_1 - g)}{g_1} \frac{(\rho_2 - \rho_1)}{(\rho_2 + \rho_1)} \right\}}. \quad (2)$$

Droplets formed from the liquid core breakup are the results of instabilities on the jet surface and leading edge, as well as initially separate from the main jet and be subjected to further breakup. Some of the larger droplets disintegrate further into smaller droplets. Droplet breakup models can be classified into three categories (Bower et al., 1988); deformation induced breakup (bag breakup), boundary layer stripping (BLS), and surface instabilities (Helmholtz and Taylor). Pilch (1981) modeled the drop breakup depending on Weber number. Droplets break up due to the bag breakup mechanism when

$$50 > We_D > 12 \quad (3)$$

where We_D is the droplet Weber number, which is the ratio of the disruptive hydrodynamic force to the surface tension force defined as

$$We_D = \frac{\rho_g U_{rel}^2 D}{\sigma_l}$$

Where ρ_g is the gas density, U_{rel} is the relative drop velocity D is drop diameter and σ_l is the

drop surface tension. Deformation of liquid drop is made by the nonuniform dynamic pressure distribution on the drop surface, and then a thin hollow bag in the center forms and grows while it is attached to a more massive toroidal rim. Bag disintegration and rim disintegration form a large number of small fragments. Droplets break up due to the sheet stripping mechanism (Pilch BLS) when

$$350 > We_D > 100. \quad (4)$$

In sheet stripping, no bags are formed; instead, a thin sheet of liquid is swept along the windward surface to the drop equator, where the sheet detaches and is carried into the wake. Beyond the sheet stripping regime, droplets break up due to the wave crest stripping and catastrophic mechanism when

$$We_D > 350. \quad (5)$$

In wave crest stripping, short-wave length, large-amplitude waves are formed on the windward surface of the drop and continuously eroded by the action of the flow field over the surface of the drops. In catastrophic breakup, long-wave length, large-amplitude waves penetrate the drop, and then create several large fragments before large portion of drop mass is reduced by wave crest stripping. Pilch (1981, 1987) insisted that *R-T* instability plays a dominant role in the acceleration driven environments. Ranger and Nicholls (1969) suggested another criteria for boundary layer stripping mechanism, where boundary layer is stripped from the periphery of the droplet due to the shearing action of the high speed gas on the droplet surface. For a given flow, droplets break up by a stripping mechanism (Ranger-Nicholls BLS; *R-N* BLS) when

$$\frac{We_D}{\sqrt{Re_D}} \gg 0.5 \quad (6)$$

where Re_D is droplet Reynolds number, defined as

$$Re_D = \frac{U_{rel} D}{\nu_l}$$

where ν_l is drop kinematic viscosity. Breakup time for BLS (Nicholls, 1972) is given as follows:

$$t = \frac{D}{U_{rel} \sqrt{\rho_g / \rho_l}} \quad (7)$$

2.2 Transient diesel breakup mode

Chang and Corradini (1991) applied the *R-T* instability, the *K-H* instability, and BLS to transient diesel fuel sprays and incorporated these models into the computer code KIVA-II (Amsden et al., 1988). In the Chang and Corradini model, the liquid column is considered as a chain of balls. They assumed that the leading edge of the balls gets high resistance from the surrounding gas while the other balls behind the leading balls get less aerodynamic resistance. At the initial stage of breakup, the leading edge of the jet is flattened by the dynamic pressure. Generally, it takes a finite time for the liquid column or larger droplet to break up. For the leading edge of the jet to be subject to possible *R-T* instability at the windward surface, the onset time of breakup (T_o^*) is expressed as follows (Simpkins and Bales, 1972):

$$T_o^* = 31 B_o^{-0.25} \quad (8)$$

where B_o is Bond number, which is the ratio of the acceleration induced body force to the surface tension force, giving

$$B_o = \frac{\rho_l a D^2}{\sigma_l}$$

where a is the drop acceleration. The Bond number is expressed in terms of drag coefficient and Weber number using the drag force relation. Newton's law for the drop can be written as follows:

$$C_D \frac{\rho_g U_{rel}^2}{2} \frac{\pi D^2}{4} = \rho_l \frac{\pi D^2}{6} a. \quad (9)$$

Dividing both sides by surface tension yields the relationship

$$B_o = \frac{3}{4} C_D We_D. \quad (10)$$

Before T_o^* is reached, Chang and Corradini applied BLS at the edge of the flattened parcel. After T_o^* is reached, they applied *R-T* instability. Once the effects of *R-T* instability manifest themselves, fragmentation occurs extremely rapidly because the growth rate of the surface waves is

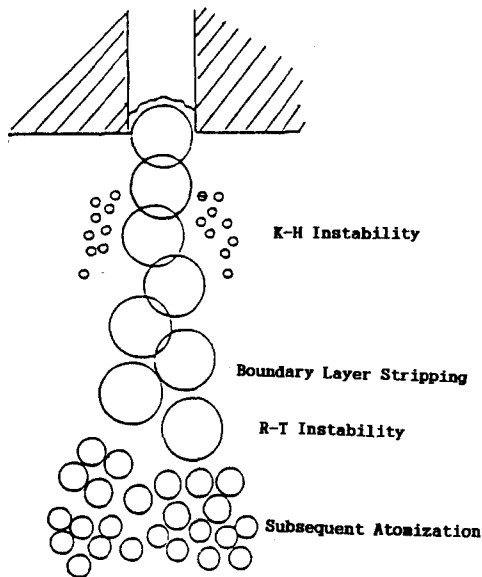


Fig. 1 Conceptual picture of breakup process

exponential.

The surface of jet column behind the leading edge is subject to the surface-wave stripping-mechanism (*K-H* instability). If the wavelength of the parcel is greater than the radius of that parcel, then this parcel has separated from the jet and excluded from the main continuous liquid core. Liquid jet column is continuously surveyed to apply breakup mechanisms. Once liquid droplets are separated from the main liquid jet column, these droplets are subjected to the single breakup mechanism. When Bond number is greater than critical Bond number, for example, (Harper et al., 1972), single droplets continue to break up by Rayleigh-Taylor instability or Kelvin-Helmholtz instability. When Bond number is less than critical Bond number and Weber number is greater than 12, single droplets may continue to break up by bag type breakup mechanism. Figure 1 shows the conceptual picture of the breakup process. Figure 2 is a block diagram of the transient breakup model.

The total dimensionless breakup time (T_b) for the R-T instability or *K-H* instability (Pilch, 1981) is defined as follows:

$$T_b = t \frac{U_{rel} \epsilon^{0.5}}{D} \quad (11)$$

Breakup Model Flow Diagram

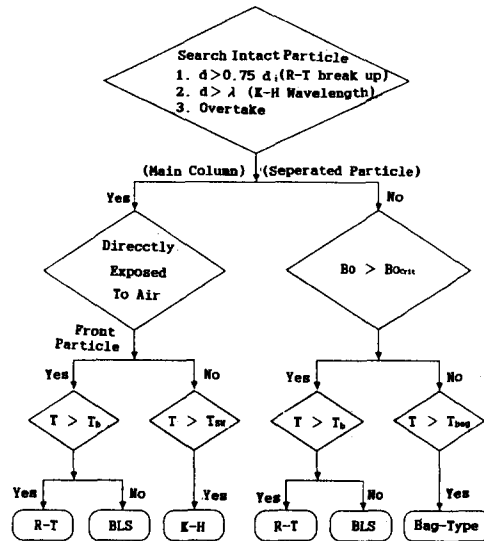


Fig. 2 Block diagram of transient breakup model

where t is the dimensional time and ϵ is flow field/droplet density ratio. Correlations for the total dimensionless breakup time (T_b) depending on the Weber number is

$$\begin{aligned} T_b &= 6.0(We - 12)^{-0.25} & 12 \leq We < 18 \\ T_b &= 2.45(We - 12)^{0.25} & 18 \leq We < 45 \\ T_b &= 14.1(We - 12)^{-0.25} & 45 \leq We < 351 \\ T_b &= 0.766(We - 12)^{0.25} & 351 \leq We < 2670. \end{aligned} \quad (12)$$

Non-dimensional drop displacement in compressible flow is

$$\bar{x} = \frac{x}{D} = \frac{3}{8} C_d T_b^2 \quad (13)$$

where C_d is drag coefficient. Drag coefficient of rigid sphere being accelerated by a compressible gas field is about 1.0 and it is about 0.5 when accelerated by incompressible gas field. However, drag coefficient of fragmenting drops are about 2 ~ 3 times larger than rigid sphere drag coefficient due to the increase of the frontal area exposed to gas field.

3. Comparison of KIVA Calculations with PDPA Data

Comparison of KIVA simulations with experi-

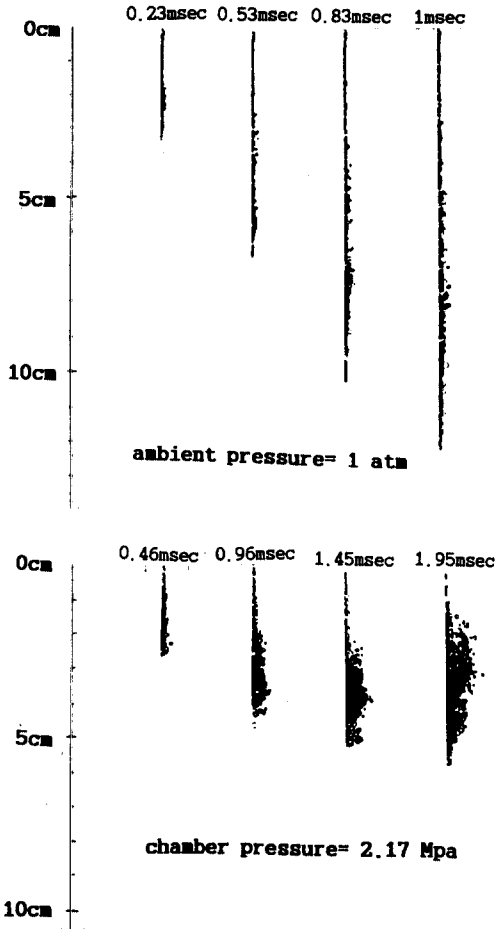


Fig. 3 Configuration of spray produced from KIVA

mental results was done in two ways. First, the computed tip penetration history was compared with measured tip penetration history. Second, the predicted droplet sizes and velocities were compared with that predicted by KIVA using Chang - Corradini breakup model. The observed tip penetration of a jet spray is a results of complex interactions between the droplets in the spray, through collisions and coalescence, atomization, other interactions between droplets and ambient gas fluid mechanics. The results from KIVA calculations presented here include the effects of entrainments, agglomeration, and spray breakup through Chang - Corradini breakup model. Spray configurations from KIVA calculations at 0.10 MPa and 2.17 MPa of ambient gas

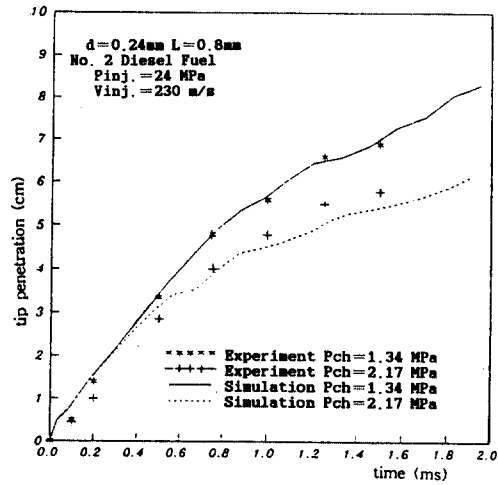


Fig. 4 Comparison of predicted tip penetration histories with measured ones

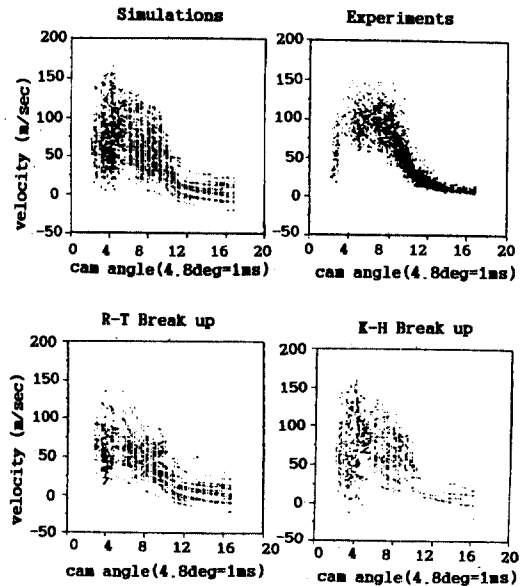


Fig. 5 Comparison of simulated velocities with measured ones using PDPA

pressure using Chang-Corradini model is shown in Fig. 3. The droplet diameters produced by KIVA was greatly magnified for presentation purpose. Comparison of the computed tip penetration history with measured tip penetration is shown in Fig. 4. The KIVA calculation initially upto 1 cm underestimates the rate of initial tip

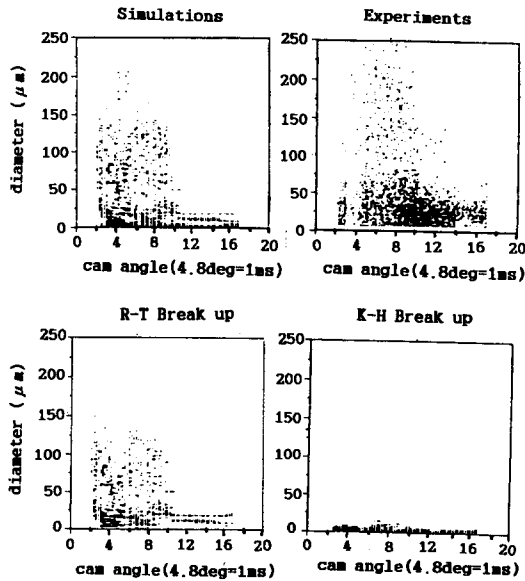


Fig. 6 Comparison of simulated droplet sizes with measured ones using PDPA

penetration. In the later part, the computed tip penetration history shows quite a good agreement with measured tip penetration. Figure 5 shows comparison of simulated drop velocities with that from PDPA at 30 mm from nozzle tip in the gas pressure of 2.17 MPa. Figure 6 shows comparison of simulated drop sizes with that from PDPA at 30 mm from nozzle tip in the gas pressure of 2.17 MPa. Droplets produced from *R-T* instability breakup model ranges small sizes to large sizes. As shown in block diagram of the transient breakup model, droplets produced from *R-T* instability is consisted of droplets from leading edge of the main column and separated large droplets. The parcels which are separated from the main column are subject to the subsequent breakup process. Droplets produced from *K-H* instability breakup model, which is only applied the jet column for surface stripping, ranges only to small sizes. This results is consistent with Taylor and Ranz's suggestion. Taylor(1963) suggested that *K-H* waves produce very fine droplets at high Weber number. Ranz(1958) proposed that ligaments and droplets are brought about by the fastest growing of the unstable surface waves. Droplet sizes are related to the unstable wave

length.

4. Spray Experimental

4.1 Experimental apparatus

The experimental apparatus used for the measurement of droplet sizes and velocities consists of spray chamber, the injection system, and the Aerometrics Phase Doppler/Particle Analyzer (PDPA). Figure 7 is a schematic diagram of the apparatus. The pumping system, injection nozzle, and instrumentation are included in the injection system. The spray, which can be pressurized to 4.1 MPa, was constructed from an aluminum cylinder, 184.25 mm I.D., 203 mm O.D., and 177 mm long. At each end of the cylinder, a flange was welded on and two circular caps were fitted to the each flange. An optical quartz window, 127 mm diameter and 25.4 mm thick, is sandwiched between two aluminum caps of 38 mm diameter at each end of the cylinder. The effective diameter of the window for optical access is 102 mm, which cover approximately 60 percent of the surface area. However the center of the optical windows is offset from the center of the main cylinder. The entire cap-optical assembly window can be rotated, which allows for views of various portions of the spray plume. In addition, the eccentric position of the quartz window allows freedom for the alignment of the PDPA. Typical of conventional injection systems, a Lucas CAV injector is connected to a Bosch model PE4P100 injection pump. A Lucas CAV, type J nozzle with a single-hole of 0.24 mm diameter and an L/d ratio of 3.33 was used in this study.

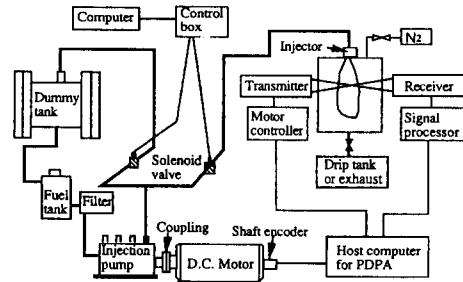


Fig. 7 Experimental apparatus

The version of the PDPA used here includes a measurement of the injector pump rotational position, such that the detailed nature of the transient events occurring in real transient fuel sprays can be studied. A 12-bit, absolute-position shaft encoder is coupled to the pump shaft to provide the digital representation of shaft position necessary for the transient spray measurements. Additional details about the experimental are available in Reference(Koo, 1991).

4.2 Application of stability criteria

Detailed measurements of droplet size and velocity at various positions and ambient gas density are compared with established stability criteria, such as bag breakup and boundary-layer stripping, in order to find where and when in the spray droplets are susceptible to breakup.

Definition of the relative velocity between the droplet and gas is critical to calculation of the breakup stability criteria. One possible choice would be to use the smallest-diameter-drop velocities as the indicator of the gas velocity. This was attempted with only limited success. Separation of the velocity according to drop-size class showed that differences were small to none in the spray axis(Koo, 1991). Thus, this procedure yielded a magnitude for the relative velocity that tended to indicate that all of the drops were stable, which cannot be true if the observed change in drop size distribution with axial position is correct. It is speculated that many of the small droplets that are measured are generated by boundary-layer stripping and/or other breakup mechanisms and are in the wake of larger drops. These droplet velocities are significantly greater than gas phase velocity. This results in velocity characteristics that are not strongly dependent on size class. To circumvent the problem of defining a precise value for the relative velocity, we have chosen two different methods to estimate the relative velocity. The two estimates have been chosen such that the true value of the relative velocity will lie somewhere between the two estimates, and the accuracy of either of the estimates depends on position and time in the fuel spray.

To produce one estimate of relative velocity, we

assume that the local gas velocity is zero. Thus the measured value of the drop velocity is taken to be the relative velocity. This, of course, produces an estimate of the relative velocity that is larger than the true value, and therefore, a higher probability of unstable droplet behavior than actually exists. However, for drops near the nozzle, in the region where the gas has just begun to accelerate, the error may not be large.

The other estimate is calculated with the assumption that the local gas velocity is equal to the mean droplet velocity. The relative velocity is then defined to be the difference between the individual drop velocity and the mean drop velocity. Here we would expect that the actual relative velocity would be larger than this value, however, for drops far from the nozzle, the entrained gas has probably been accelerated up to the mean drop velocity. Near the nozzle, this estimate is most likely much too small.

The relative velocities ($|U_{drop} - U_{mean}|$) necessary to have a droplet Weber number equal to the critical value of 12, 100, 350, and to meet the BLS criterion, which are shown in Eqs. (3)~(6), are plotted in Fig. 8. Relative velocity line from R-N BLS in Fig. 8 is lower than that obtained from Pilch BLS. This confirms that R-N BLS occurs when is much greater than 0.5 as expressed in Eq. (6). For small drop sizes at lower gas densities and large drop sizes at higher gas densities, the

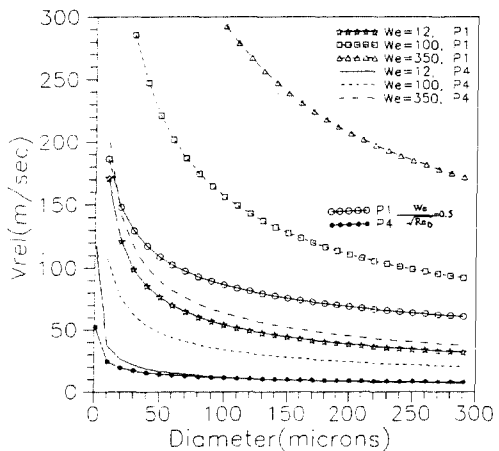


Fig. 8 Relative velocities for various stability criteria versus drop diameter

bag breakup and R-N BLS stability curves showed little difference, in contrast to a noticeable difference in large size/lower density and small size/higher density case.

Drag coefficient for fragmenting drops in compressible flow(Pilch, 1981) is about 2.5. When T_b has 6.0 ($We=12$), drop displacement(\bar{x}) is 33.8. The droplet size of $100 \mu\text{m}$ moves 3.3 mm before complete breakup. When T_b is 3,3 ($We=350$), droplet size of $100 \mu\text{m}$ moves 1.0 mm before breakup. These stability criteria can be applied to the actual data as shown in Figs. (8)~(9). The axes represent U_{rel} and drop diameter, meaning that each of the stability limits forms a hyperbola. Individual drop size/velocity pairs are plotted as individual points. Data that lie above and to the right of the lines defining the stability limits are assumed to be unstable and will experience breakup. Data that lie below or to the left of the stability limits should be stable to that form of breakup.

Four different cases are presented to demonstrate the effect of position in the spray. Comparisons are shown in Fig. 9 ($x=10 \text{ mm}$, $r=0 \text{ mm}$, $r=1 \text{ mm}$) for the spray axis and Fig. 10 ($x=60 \text{ mm}$, $r=0 \text{ mm}$, $r=7 \text{ mm}$) for edges of the spray .

At a position 10 mm from the nozzle tip, right on the axis of the spray, the tendency for droplet breakup is dependent on the definition of the relative velocity. If the definition for relative velocity was used, 55.7 percent of the droplets in Fig. 9(a) is susceptible to bag breakup, while 55.9 percent would be susceptible to boundary layer stripping. If the $|U_{drop} - U_{mean}|$ relative velocity is equal to the measured value, 77.8 percent of the droplets in Fig. 9(b) is susceptible to bag breakup, while 80.8 percent would be susceptible to boundary layer stripping. Thus, the data shown in Fig. 9(a) exhibit indicate that more than 55% of drops are at least unstable at this position. For droplets near the nozzle, however, more appropriate definition of relative velocity is using drop velocity itself rather $|U_{drop} - U_{mean}|$ because the gas has just begun to accelerate. Then, the data shown in Fig. 9(b) exhibit indicate that more than 77% of drops are a unstable at this position, the error may not be large. At spray axis in downstream, using the definition of $|U_{drop} - U_{mean}|$ as relative velocity, approximately 89% are stable to bag breakup and 86% are stable to boundary layer stripping in Fig. 9(c). If the relative velocity is equal to the measured value, approximately 53%

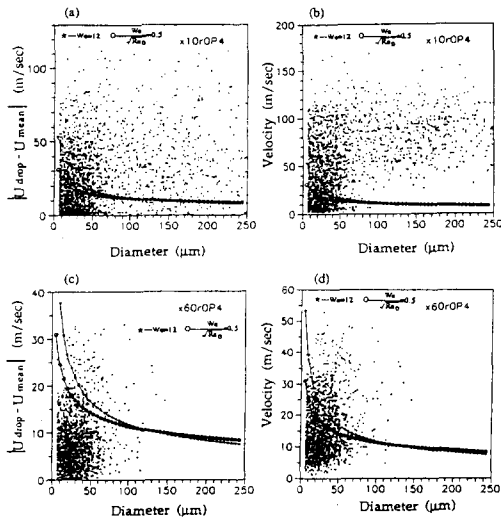


Fig. 9 Comparison of individual droplet velocity and diameter with stability criteria for bag breakup and BLS at spray axis ($x=10$, $r=0$ and $x=60$, $r=0$). $P_{gas}=2.17 \text{ MPa}$

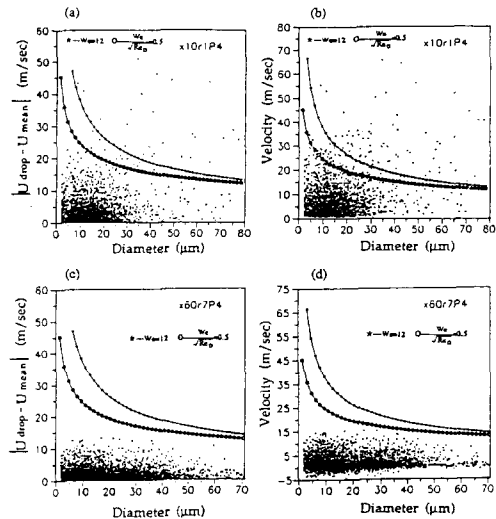


Fig. 10 Comparison of individual droplet velocity and diameter with stability criteria for bag breakup and BLS at spray edges ($x=10$, $r=1$ and $x=60$, $r=7$). $P_{gas}=2.17 \text{ MPa}$

are stable to bag breakup and 47% are stable to boundary layer stripping in Fig. 9(d). From the data shown in Fig. 9(c) and (d), we would expect that a more appropriate measure of the relative velocity would be the $|U_{drop} - U_{mean}|$, because the gas has had sufficient time to come to equilibrium with the average jet or droplet velocity. Thus, the data shown in Fig. 9(c) and (d) exhibit little tendency for either type of breakup, indicating mostly stable drops at this position. The data shown in Fig. 10(a)~(d) are similar, except that here ($x=60$ mm, $r=0$ mm, $r=7$ mm) we would expect that a more appropriate measure of the relative velocity would be the $|U_{drop} - U_{mean}|$, because the gas has had sufficient time to come to equilibrium with the average jet or droplet velocity. Thus, the data shown in Fig. 10(a) exhibit little tendency for either type of breakup, indicating mostly stable drops at this position (97.8% drops are stable for bag type, 96.8 for BLS). In the downstream and spray edge regions in Fig. 10(c) and (d), all the droplets are stable no matter which stability criterion is applied.

5. Conclusion

From a new liquid jet breakup model which is incorporated into the KIVA-II code, the configuration of transient spray can be predicted. Liquid column is considered as a chain of balls. After reaching at breakup time, Rayleigh-Taylor instability was applied to the leading edge of the jet and Kelvin-Helmholtz instability to the surface of jet column, contrasting that boundary stripping mechanism is used before breakup time. Computational results using the proposed models in the KIVA-II program showed a reasonable agreement with the PDPA measurement data. Comparison with the stability criteria and KIVA calculations indicate that a majority of the droplets in the spray are susceptible to both breakup mechanisms near the nozzle region. However, the spray appears to stabilize on the spray edge and downstream.

Acknowledgement

We express our thanks to professors Martin and Corradini for their helpful suggestions and guidance. Partial support for this work came from Engine Research Center of UW-Madison and Advanced Fluids Engineering Research Center of KOSEF.

References

- Amsden, A. A., O'ourke, P. J. O. and Butler, T. D., 1989, "KIVA-II: A Computer Program for Chemically Reactive Flows With Sprays," LA-11560-MS.
- Bower, G. R., Chang, S. K., Corradini, M. L., El-Beshbeeshy, M., Martin, J. K. and Krueger, J., 1988, "Physical Mechanisms for Atomization of a Jet Spray: A Comparison of Models and Experiments," *SAE Trans.*, Vol. 97, SAE Paper No. 881318.
- Chandrasekhar, S., 1971, "Hydrodynamic and Hydromagnetic Instability," Oxford Press, pp. 481~512
- Chang, S. K., 1991, "Hydrodynamics of Liquid Jet Sprays," Ph. D. Thesis, University of Wisconsin-Madison.
- Harper, E. Y., Grube, G. W. and Chang, I. -D., 1972, "On the Breakup of Accelerating Liquid Drops," *J. Fluid Mech.*, Vol. 52, Part 3, pp. 565~591.
- Hiroyasu, H. and Arai, M., 1990, "Structures of Fuel Sprays in Diesel Engines," SAE paper 900475.
- Koo, J. Y., 1991, "Characteristics of a Transient Diesel Fuel Spray," Ph. D. Thesis, University of Wisconsin-Madison.
- Lord Taylor, F. R. S., 1878, "On the Instability of Jets," *Proc. Lond. Math. Soc.*, Vol. 4, pp. 4~13.
- Nicholls, 1972, "Stream and Droplet Breakup by Shock Wave," *NACA SP-194*, pp. 126~128.
- Pilch, M. and Erdman, C. A., 1987, "Use of Breakup Time Data and Velocity History Data to Predict the Maximum Size of Stable Fragments for Acceleration-Induced Breakup of a Liquid

Drop," *Int. J. Multiphase Flow*, Vol. 13, No. 6, pp. 741~757.

Pilch, M., 1981, "Acceleration Induced Fragmentation of Liquid Drops," Ph. D. Thesis, University of Virginia.

Ranger, A. A. and Nicholls, J. A., 1969, "Aerodynamic Shattering of Liquid Drops," *AIAA Journal* Vol. 7, No. 2, pp. 285~289.

Ranz, W. E., 1958, "Some Experiments on Orifice Sprays," *Can. J. Chem. Eng.* Vol. 35, pp. 175~181.

Reitz, R. D., 1978, "Atomization and Other Breakup Regimes of a Liquid Jets," Ph. D. Thesis, Princeton University, Department of Aerospace Engineering, 1375-T.

Reitz, R. D. and Bracco, F. V., 1979, "On the Dependence of Spray Angle and Other Spray

Parameters on Nozzle Design and Operating Conditions," SAE paper 790494.

Ruiz, F. and Chigier, N., 1985, "The Mechanism of High Speed Atomization," ICLASS-85, London.

Simpkins, P. G. and Bales, E. L., 1972, "Water-Drop Response to Sudden Accelerations," *J. Fluid Mech.*, Vol. 55, Part 4, pp. 629~639.

Taylor, G. I., 1963a, "Generation of Ripple by Blowing over a Viscous Fluid," *The Scientific Papers of G.I. Taylor*, edited by Batchelor, G. K., Cambridge University Press Vol. 3, pp. 244~254.

Taylor, G. I., 1963b, "The Instability of Liquid Surfaces When Accelerated in a Direction Perpendicular to Their Planes. I," *The Scientific Papers of G. I. Taylor*, edited by Batchelor, G. K., Cambridge University Press Vol. 3, pp. 532~536.